

# Asymmetry of Electron Transmission through Monolayers of Helical Polyalanine Adsorbed on Gold Surfaces

Slawomir Sek,\* Anna Tolak, Aleksandra Misicka, Barbara Palys, and Renata Bilewicz

Department of Chemistry, University of Warsaw, Pasteura 1, 02093 Warsaw, Poland

Received: April 26, 2005; In Final Form: July 28, 2005

Polyalanine derivatives containing cysteamine linker  $R-(\text{Ala})_{14}\text{NH}-(\text{CH}_2)_2-\text{SH}$ , where R is ferrocenecarbonyl or hydrogen, were synthesized and then used to form self-assembled monolayers on gold. The tilt angles and the packing density of the molecules within monolayer assemblies were determined by FTIR spectroscopy and scanning tunneling microscopy, respectively. Electrochemical properties of monolayer-modified electrodes were studied using cyclic voltammetry and impedance spectroscopy. Measurements of electron-transfer rates using electrochemical techniques and scanning tunneling spectroscopy revealed asymmetry dependent on the applied voltage. It is suggested that the observed electron-transfer behavior is connected with the electric field generated by the molecular dipole of the polyaniline helix.

## Introduction

Electron-mediating properties of organic molecules remain a point of interest in nanotechnology and construction of molecular devices.<sup>1</sup> The ability of oligopeptides and polypeptides to transfer electrons at long distances has been shown recently by several groups. The electron-transfer (ET) investigations included spectroscopy,<sup>2</sup> electrochemical studies,<sup>3–8</sup> and conductance studies using scanning tunneling microscopy (STM).<sup>9</sup> It was reported that the electron transfer through peptides occurs according to the tunneling mechanism for shorter bridges, while for the longer peptide chains the electron hopping contributes to the overall process.<sup>2,4,10</sup> These results are supported by the theoretical calculations carried out by Petrov and May.<sup>11</sup> On the other hand, some recently reported experimental results obtained for oligopeptides containing  $\alpha$ -aminoisobutyric acid units by Maran and co-workers do not confirm an electron-hopping contribution to ET through peptides.<sup>3</sup> The authors postulated that the unusually smooth distance dependence of rate constants observed in their experiments results from the increase of electronic coupling due to the lowering of the energy of the bridge in the presence of hydrogen bonds. This effect counteracts the usual rate decrease expected for a superexchange mechanism.

Results of several electron-transfer studies through polypeptides and proteins suggest that the efficiency of electron transport is strongly influenced by the length of the peptide, the nature of the scaffold, and the amino acid sequence.<sup>7,10,12,13</sup> The presence of hydrogen bonding also influences the electron-transfer rates.<sup>14–17</sup> In the case of  $\alpha$ -helical peptides containing  $\alpha$ -aminoisobutyric acid and alanine units, the electron transfer may be strongly affected by the molecular dipole of the helix.<sup>18</sup> It is known that helical peptides have large dipole moments oriented along the molecular axis. When the direction of the electron transfer is aligned with the field generated by the dipole, the electron-transfer rates are usually faster than the electron-transfer rates for the direction against the dipole, as found by time-resolved fluorescence measurements for dichromophoric

$\alpha$ -helical peptides.<sup>18</sup> The propensity of helical peptides to modulate the electron-transfer rate was recently utilized by Kimura and co-workers to obtain a photodiode system, in which two molecular photodiodes generate photocurrent along the molecules in opposing directions.<sup>19</sup> In this case, the photodiode system was based on mixed self-assembled monolayers (SAMs) of two helical peptides containing  $\alpha$ -aminoisobutyric acid and leucine units. Here we report the electrochemical and scanning tunneling spectroscopy (STS) studies of electron transfer through self-assembled monolayers formed by thiolated polyaniline derivatives. It is well-known that thiol compounds can form highly ordered SAMs on gold by covalent Au–S linkage.<sup>20,21</sup> Purposely modified molecules used to form self-assembled monolayers allow one to control the structure and the properties of the system. Using peptide chains with thiol functions, the monolayers can be considered as simple models of biological systems. In this paper we report the electron-transfer properties of polyaniline with a cysteamine linker adsorbed on gold surface. The efficiency of electron transport through peptide molecules was studied using electrochemical techniques and scanning tunneling spectroscopy. Alanine is one of the helix-favoring amino acids.<sup>22</sup> Therefore, in the case of polyaniline used in the present work  $\alpha$ -helix structure is dominating. We show the asymmetry of the electron-transfer rates and describe it by means of changes of electric field generated by the molecular dipole of the helix.

## Experimental Section

**Chemicals.** Ethanol, perchloric acid, and potassium hydroxide were purchased from POCh Gliwice. All other compounds used in this work were purchased from Sigma-Aldrich and Merck. Water was distilled and passed through a Milli-Q purification system. The final resistivity of water was  $18.2 \text{ M}\Omega \cdot \text{cm}^{-1}$ .

**Synthesis.** The synthesis of an electroactive derivative of polyaniline, namely,  $\text{Fc}-(\text{Ala})_{14}\text{NH}-(\text{CH}_2)_2-\text{SH}$ , was performed manually by solid-phase synthetic techniques starting from 0.31 mmol/g of commercially available cysteamine 4-methoxytrityl resin (Novabiochem). Successively,  $N^{\alpha}$ -fluorenylmethoxycarbonyl (Fmoc) protected alanine (Novabiochem) and ferrocenecarboxylic acid (Sigma) were coupled using

\* To whom correspondence should be addressed. E-mail: slasek@chem.uw.edu.pl.

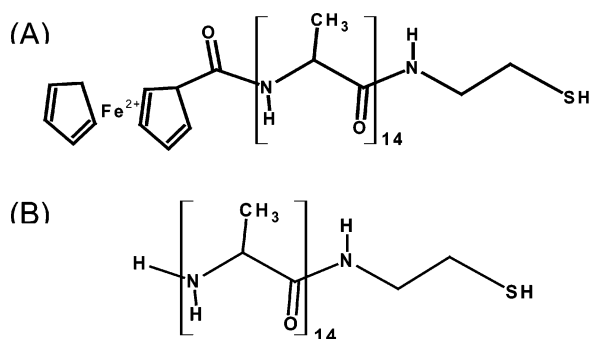


**Figure 1.** Molecular structure of polyalanines: Fc-(Ala)<sub>14</sub>NH-(CH<sub>2</sub>)<sub>2</sub>-SH (A) and H-(Ala)<sub>14</sub>NH-(CH<sub>2</sub>)<sub>2</sub>-SH (B).

*N*-hydroxybenzotriazole (Aldrich) and diisopropylcarbodiimide (Aldrich) as coupling reagents. Each coupling reaction was monitored by qualitative ninhydrine test and repeated until the test was negative. The cleavage of final product was performed by 5% trifluoroacetic acid (Aldrich) in dichloromethane (POCH Gliwice) containing 5% triisopropylsilane (Sigma). The final product was purified by preparative RP-HPLC and then analyzed by ESI-MS ( $[M + Na]^+$ <sub>calc</sub> = 1306.5;  $[M + Na]^+$ <sub>found</sub> = 1306.3).

**Preparation of Electrodes.** Monolayer-modified Au(111) substrates (Arrandee) were used as working electrodes. The substrates were 200–300 nm thick gold films evaporated onto borosilicate glass precoated with 1–4 nm underlayer of Cr. Before the deposition of the monolayer, the substrates were cleaned by etching for 5–10 min in hot nitric acid and then flame annealed until the sample glowed dark red. Then the substrate was cooled to room temperature. After the annealing procedure the substrates were transferred to a coating solution. Self-assembly was carried out from 1 mM ethanol solutions. In the case of mixed monolayer, the solution contained 0.05 mM of polyalanine derivative and 0.95 mM of octadecanethiol. After 18 h of being soaked, the substrates were washed with ethanol and water. Fresh samples were prepared before each experiment.

**Electrochemistry.** Electrochemical experiments were carried out in a three-electrode cell with Ag wire as a reference electrode and platinum foil as a counter electrode. The supporting electrolyte was 1 M HClO<sub>4</sub> or 1 M KOH (in the case of desorption experiments). The measurements were performed using Autolab PGSTAT30 and CHI660A potentiostats. All electrochemical experiments were carried out at 25 °C.

**Infrared Spectroscopy.** Infrared spectroscopy was performed with FTIR 8400 Shimadzu equipped with specular reflectance accessory—SpectraTech at 82° angle of incidence. The polarized light was used. Spectra were collected as 1000 averaged scans.

**Scanning Tunneling Microscopy.** STM and STS measurements were performed using a Nanoscope IIIa (Digital Instruments, Santa Barbara, CA) equipped with a low-current converter. The images and the STS data were taken under ambient conditions in air with commercially available Pt–Ir tips (Nanotips, Digital Instruments). The images were acquired using constant-current mode.

## Results and Discussion

**Two-Component Electroactive SAM.** Mixed monolayers contained ferrocene derivative of polyalanine as an electroactive component and *n*-octadecanethiol as diluent for redox molecules. The chemical structure of the electroactive derivative of polyalanine (Fc-(Ala)<sub>14</sub>NH-(CH<sub>2</sub>)<sub>2</sub>-SH) is shown in Figure 1A. Two-component monolayers on gold were characterized by

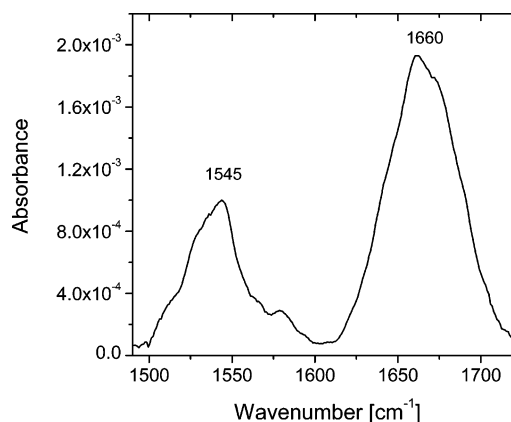


**Figure 2.** Amide region of infrared spectra recorded for self-assembled monolayers of electroactive polyalanine and octadecanethiol.

reflectance infrared spectroscopy and electrochemical methods, i.e., cyclic voltammetry and electrochemical impedance spectroscopy. The amide region of surface FTIR spectra recorded for mixed SAM is shown in Figure 2. The information about the structure of the monolayer assembly can be extracted from the position and the intensity of amide bands.<sup>4,23,24</sup> Amide I and amide II bands of the polyalanine appear at 1660 and 1545 cm<sup>-1</sup>, respectively, which indicates that  $\alpha$ -helical conformation is a dominating structure within the peptide chains.<sup>23,24</sup> On the basis of the absorbance intensity ratio of amide I/amide II bands in the IR spectra, we calculated the tilt angle of the helix axis from the surface normal. The molecular orientation of the molecules on gold surface was determined according to the following equation:<sup>23</sup>

$$\frac{I_1}{I_2} = 1.5 \times \frac{(3 \cos^2 \gamma - 1)(3 \cos^2 \theta_1 - 1) + 2}{(3 \cos^2 \gamma - 1)(3 \cos^2 \theta_2 - 1) + 2} \quad (1)$$

where  $I_{1,2}$  represent the observed absorbances of amide I and amide II bands,  $\gamma_{1,2}$  are the tilt angles of the helical axis from the surface normal, and  $\theta_{1,2}$  represent the angles between the transition moment and the helix axis. The values of  $\theta_1$  and  $\theta_2$  were taken to be 39 and 75°, respectively.<sup>23</sup> The value of the tilt angle of the helix from the surface normal was found to be  $47 \pm 2^\circ$ . In this calculation we assumed the uniform orientation of the helix axis around the surface normal. Therefore the result should be considered as an estimated value since the existence of the fraction of molecules with different secondary structure features, such as  $3_{10}$ -helix or  $\beta$ -turns, cannot be completely excluded.

A typical cyclic voltammogram recorded for the two-component monolayer of polyalanine derivative and octadecanethiol is shown in Figure 3. Two peaks correspond to the one-electron redox process of the Fc/Fc<sup>+</sup> couple. The relationship between peak currents and the scan rates was linear, which indicated that electron transfer originates from the surface-bound redox center. The surface coverage of polyalanine derivative molecules was estimated from the area of the cyclic voltammetric peaks corresponding to the oxidation of ferrocene centers and found to be  $7.4 \times 10^{-12}$  mol/cm<sup>2</sup>. If we consider that the maximum coverage of Fc-(Ala)<sub>14</sub>NH-(CH<sub>2</sub>)<sub>2</sub>-SH,  $\Gamma$ , is equal to  $3.1 \times 10^{-10}$  mol/cm<sup>2</sup>, the value given above corresponds to 2% content of the electroactive component within the monolayer.<sup>25</sup> The capacitances of monolayer-modified electrodes were measured using electrochemical impedance spectroscopy at the potential corresponding to the double layer region, i.e., 0 V. The frequency range for these measurements was from 0.1 Hz

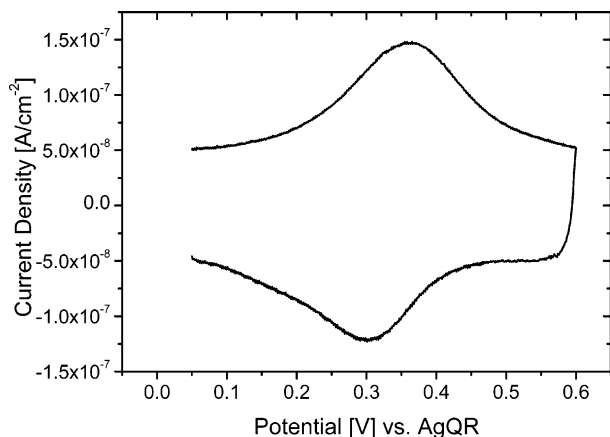


**Figure 3.** Typical cyclic voltammogram obtained in 1 M HClO<sub>4</sub> for gold electrode modified with mixed monolayers of electroactive polyaniline and octadecanethiol.

to 100 kHz, and the equivalent circuit used to calculate the capacitances included the resistor and capacitor connected in the series. The value of double-layer capacitance reflects the order of the monolayer and its permeability toward electrolyte ions and solvent molecules.<sup>26</sup> We found that the mean value of capacitance for gold electrodes coated with mixed monolayers of electroactive polyaniline and octadecanethiol was  $2.5 \pm 0.4 \mu\text{F}/\text{cm}^2$ , which is higher than for the one-component monolayer of octadecanethiol on gold.<sup>27</sup> The difference in capacitance is due to the presence of polyaniline molecules, which have higher polarity compared to simple alkanethiols. As it was already mentioned, alanine is one of the helix-favoring residues. Therefore, the  $\alpha$ -helix structure prevails in the case of polyaniline. It is known that  $\alpha$ -helical peptides have large dipole moments (about 3.5 D/residue) oriented along the molecular axis. It means that the dipole moment for polyaniline containing 14 alanine residues is larger than 40 D, while in the case of simple *n*-octadecanethiol molecule the dipole moment is about 1.5 D. This may explain the difference between the double-layer capacitances observed for the two types of monolayers. Another explanation involves water molecules, which can reside inside the monolayer close to the peptide bonds.

In the case of the mixed monolayers we investigated the rates of electron-transfer mediated by polyaniline bridge. The rate constants were determined from cyclic voltammograms. At any point of the voltammogram, the instantaneous faradaic current is given by<sup>28</sup>

$$i_f = nFA(k_a\Gamma_{\text{Red}} - k_c\Gamma_{\text{Ox}}) \quad (2)$$

where  $n$  is the number of electrons,  $F$  is the Faraday constant,  $A$  is an area of the electrode,  $k_a$  and  $k_c$  are the rate constants of anodic and cathodic process, and  $\Gamma_{\text{Red}}$  and  $\Gamma_{\text{Ox}}$  are the surface concentrations of redox centers in reduced or oxidized state. If the potential is at least 60 mV beyond the formal potential of the redox couple, the equation given above reduces to<sup>28</sup>

$$i_f = kQ(t) \quad (3)$$

where  $k = k_a$  for oxidation,  $k = k_c$  for reduction, and  $Q(t)$  is the charge density corresponding to the quantity of unreacted redox sites on the electrode. The rate constant at given overpotential can be calculated by dividing the instantaneous faradaic current by  $Q(t)$  for that potential. The standard rate constant is determined from a Tafel plot by extrapolation of  $\ln k$  to zero overpotential. The standard rate constant for electron transfer through polyaniline was found to be  $k^0 = 0.30 \pm 0.08 \text{ s}^{-1}$ .

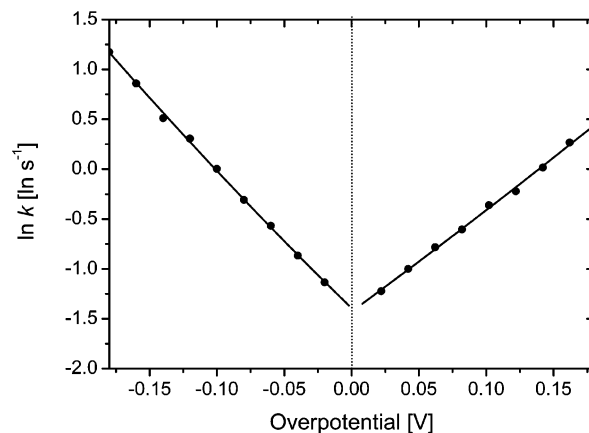


**Figure 4.** Tafel plot at low overpotentials obtained for mixed SAMs of electroactive polyaniline and *n*-octadecanethiol.

If we assume that the electron transfer occurs according to the tunneling mechanism, it is possible to estimate the tunneling coefficient  $\beta$  using the following equation:<sup>29</sup>

$$k = k_0 \exp(-\beta d) \quad (4)$$

where  $k$  is the rate constant for electron transfer mediated by molecular bridge,  $k_0$  is the rate constant in the absence of the molecular bridge, and  $d$  is the length of the molecular bridge. In our case, the theoretically predicted length of the polyaniline spacer is  $28.5 \text{ \AA}$ .<sup>30</sup> Using the values of the standard rate constants obtained from our experiments and assuming  $k_0 = 3 \times 10^8 \text{ s}^{-1}$ ,<sup>31</sup> we calculated the tunneling coefficient  $\beta = 0.73 \pm 0.01 \text{ \AA}^{-1}$ , which is slightly lower than  $1.0 \text{ \AA}^{-1}$  reported for *n*-alkyl bridges.<sup>32</sup> It means that the electron tunneling through helical peptide may be more efficient than through simple alkyl chains.

The analysis of the kinetics of electron transfer through helical peptide reveals an interesting feature. The Tafel plots constructed from cyclic voltammograms show small but visible asymmetry (Figure 4). It is known that the electron-transfer rate through  $\alpha$ -helical peptides is influenced by electric field generated by the dipole of the helix.<sup>4,18,33</sup> In  $\alpha$ -helical peptides, the dipole moments of amino acid residues are oriented in the same direction, almost parallel to the helix axis. The resulting dipole of the helix produces an effective positive charge at the N-terminus, and the effective negative charge at the C-terminus influencing the electron-transfer rates which are observed for  $\alpha$ -helical peptides.<sup>4,18,33</sup> The visible asymmetry of Tafel plots observed in our studies is probably connected with this effect, since at the positive overpotentials electrons are transferred from ferrocene moiety to gold electrode (oxidation process described by rate constant  $k_a$ ), while for negative overpotentials the direction of electron transfer is opposite (reduction process described by rate constant  $k_c$ ). It means that in our case the electrons are transferred from N-terminus to C-terminus for positive overpotentials, while for negative overpotentials the electron-transfer direction is from the C-terminal end to the N-terminal end (Figure 5). The electron-transfer rates through polyaniline derivative monolayer are increased for negative overpotentials; thus the rate constant  $k_c$  is higher than  $k_a$  at given absolute value of overpotential. The average ratio of rate constants  $k_c/k_a$  was  $1.43 \pm 0.07$ . This value is not as large as that observed in time-resolved fluorescence measurements for dichromophoric  $\alpha$ -helical peptides (in this case the ratio ranged from 5 to 27),<sup>18,33</sup> but it should be noted that the effect of molecular dipole depends on the solvent.<sup>33</sup> Increase of solvent



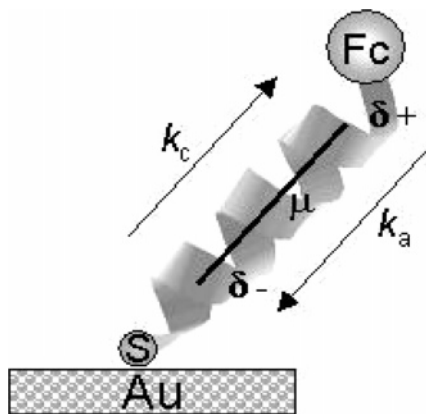


**Figure 5.** Scheme illustrating directional dependence of electron transfer through polyaniline derivative.

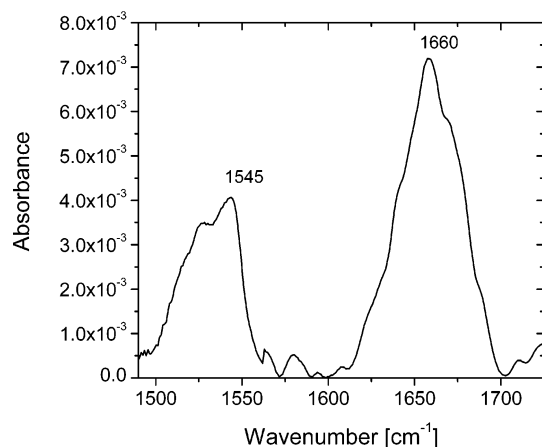


**Figure 6.** Amide region of infrared spectra recorded for the self-assembled monolayer of nonelectroactive polyaniline.

polarity reduces the effect of molecular dipole due to the solvation of amino acid residues. In our case the peptide bridge can be solvated by water molecules, which results in dampening of the molecular dipole effect.

**One-Component Nonelectroactive SAM.** Gold substrates coated with one-component monolayers of nonelectroactive polyaniline  $\text{H}-(\text{Ala})_{14}\text{NH}-(\text{CH}_2)_2-\text{SH}$  (see Figure 1B) were characterized by reflectance infrared spectroscopy, electrochemical methods, and scanning tunneling microscopy.<sup>34</sup> The amide region of surface FTIR spectra recorded for one-component SAM is shown in Figure 6. In this case, the amide I and amide II bands of polyaniline appear at 1660 and 1545  $\text{cm}^{-1}$ , respectively, which also confirms that  $\alpha$ -helical conformation is a dominating structure within the peptide chains.<sup>4,23,24</sup> The tilt angle of the helix axis from the surface normal was found to be about  $48 \pm 3^\circ$ .

The surface coverage of nonelectroactive polyaniline was estimated from the charge corresponding to the reductive desorption of thiolates from the gold surface. Desorption experiments were performed in 1 M KOH aqueous solution. The typical cyclic voltammogram curve obtained in these experiments is shown in Figure 7. When the gold electrode modified with thiol monolayer is immersed in alkaline solution and the potential is swept to sufficiently negative value, a reduction peak appears, which corresponds to the reductive desorption of the thiol molecules from the electrode surface.<sup>35</sup> Assuming that one electron is involved in this process, the surface coverage of the electrode calculated from the peak area (i.e. charge associated with reduction process) was found to be equal to  $(3.7 \pm 1.0) \times 10^{-10} \text{ mol/cm}^2$ . This corresponds to the mean molecular area

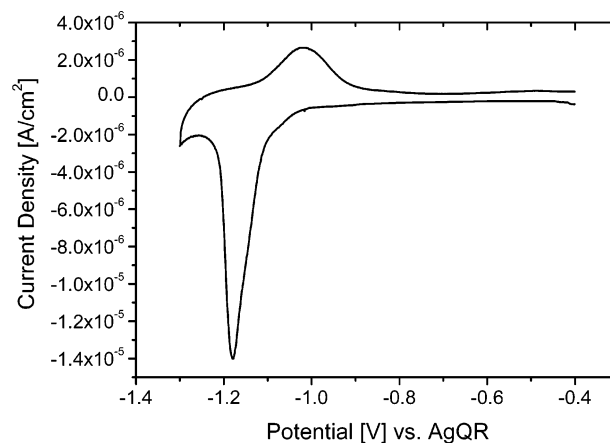


**Figure 7.** Electrochemical desorption of the monolayer of nonelectroactive polyaniline. The curve was recorded in 1 M KOH.

of 45  $\text{\AA}^2$ . The capacitance of the electrodes coated with nonelectroactive polyaniline was measured as previously done, using electrochemical impedance spectroscopy at the potential 0 V. The mean value of capacitance for modified gold electrodes was  $3.2 \pm 0.7 \mu\text{F/cm}^2$ . The STM image in Figure 8 shows that nonelectroactive polyaniline molecules can form well-ordered domains on gold surface with an intermolecular distance  $8 \pm 1 \text{ \AA}$ , which corresponds to the mean molecular area of 54  $\text{\AA}^2$ . This area is larger than the result obtained from the electrochemical desorption experiment, which is reasonable if we consider that the latter was calculated from the charge, which is usually overestimated due to the double-layer charging during the desorption process. One should note that the mean molecular area calculated from desorption experiments and from STM data actually provides the information about the spacing between neighboring molecules; thus, the values of mean molecular area given above are not equivalent with projected molecular area.

In the case of one-component monolayers of nonelectroactive polyaniline, electron transfer was studied using scanning tunneling spectroscopy. These experiments were performed in air under ambient conditions. The electrical behavior of the monolayers was examined as a function of the tip–substrate distance at fixed bias voltage. In this experiment, the current was measured when the STM tip was lowered toward the surface of the modified gold substrate.<sup>36</sup> The STS data were taken over the well-ordered domains of the monolayer assembly. At the beginning, when the tip was sufficiently far from the surface of the monolayer, we observed small currents comparable to the noise. When the tip started to penetrate the monolayer, the current increased exponentially with decreasing gap between the tip and the Au substrate, according to the following empirical equation:<sup>36</sup>

$$i = i_{d=0} \exp(-\beta d) \quad (5)$$

where  $d$  is the distance between the tip and the substrate,  $\beta$  is the tunneling coefficient,  $i$  is the current measured in the presence of the monolayer, and  $i_{d=0}$  is the current in the absence of the film measured at  $d = 0$ . Thus, from the slope of the  $\ln i$  vs  $d$  curve (Figure 9) we obtain the tunneling coefficient  $\beta$  for the polyaniline SAM,  $\beta = 0.69 \pm 0.12 \text{ \AA}^{-1}$ . The value of the tunneling coefficient was determined on the basis of 50 individual experiments performed on five independently prepared samples. The method described above cannot be, however, considered as a very accurate determination of  $\beta$ , because the results are strongly influenced by changes in the secondary structure of the peptide molecules. In this experiment some

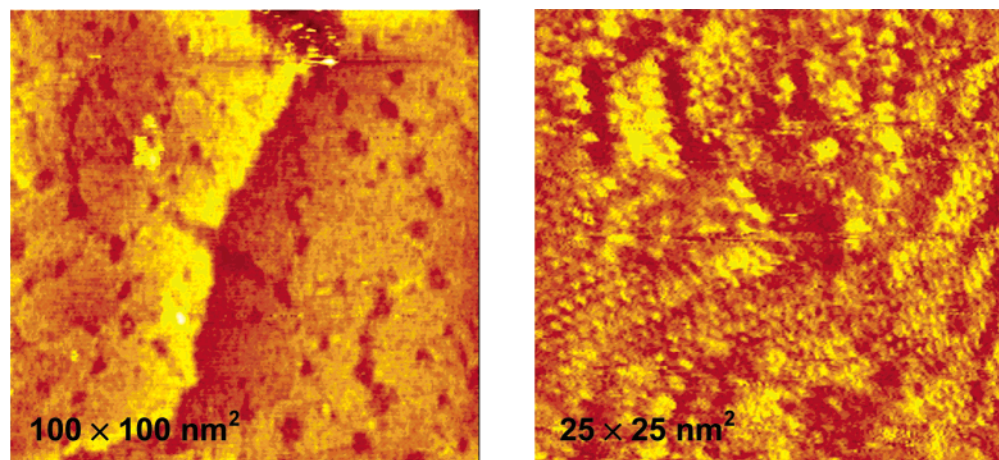


**Figure 8.** STM image of the self-assembled monolayer of nonelectroactive polyaniline. The images were taken at a tunneling current of 1 pA and the bias voltage of 1 V.

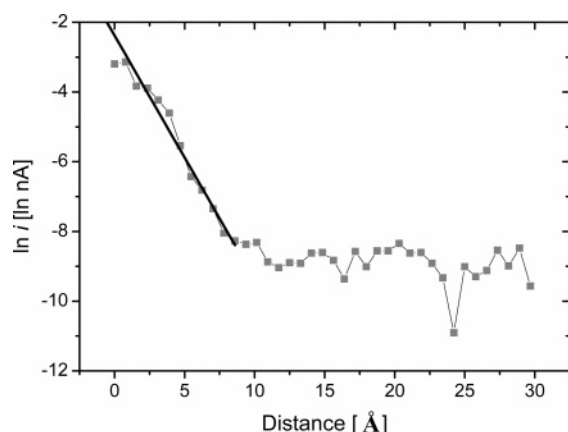


**Figure 9.** Example of current vs distance curve recorded for the gold substrate coated with the monolayer of nonelectroactive polyaniline. Current is plotted on a natural logarithmic scale: tip bias, 1.0 V.

molecules forming the SAM are probably “squeezed” between the tip and the substrate, which is reasonable if we consider that the tip partially penetrates the monolayer. Thus, we expect that the secondary structure of the peptide may not be preserved during this measurement. On the other hand, the result obtained from the STS measurement is relatively close to that estimated from electrochemical data.

The electrical properties of the nonelectroactive polyaniline SAM were also investigated as a function of bias voltage at a fixed distance between the tip and the substrate.<sup>37</sup> These experiments were also performed in air under ambient conditions. As previously, the STS data were taken over a well-ordered domain of the monolayer assembly. The analysis of the data was performed on the basis of 56 individual measurements on five independently prepared samples. The examples of  $i$ - $V$  curves are shown in Figure 10. The STS data reveal an asymmetry in the tunneling spectra. The currents at positive bias voltage were usually 2–3 times smaller than the currents at negative bias. The average ratio of the positive current to negative current was  $2.4 \pm 0.3$ . This result seems to confirm our earlier observations. As described above, the Tafel plots obtained for mixed SAM show small but visible asymmetry, probably due to the electric field generated by the molecular dipole of the helix. In the case of the STS data, the same effect may be responsible for the asymmetry of  $i$ - $V$  curves. It is reasonable if we consider that the directional dependence of electron transfer is exactly the same as we observed in electrochemical experiments. Lower currents were recorded at

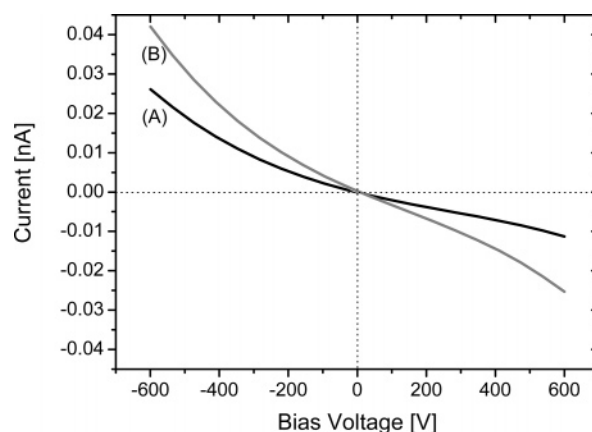


**Figure 10.** STS data recorded for the gold coated with the monolayer of nonelectroactive polyaniline. The curves were recorded at the current set points of 10 (A) and 25 pA (B). Bias set point was 0.6 V.

positive bias voltage, which induces negative tunneling currents. It means that the electrons flow from the tip to the substrate. Thus, the electrons are transferred in the opposite direction with respect to the molecular dipole. At negative bias the electrons flow from the substrate to the tip, i.e., along the molecular dipole of the helix; therefore, the currents are larger.

## Conclusions

Directional dependence of electron transfer is shown by electrochemical methods for the organothiol monolayers containing polyaniline molecules with electroactive ferrocene groups and for the nonelectroactive monolayers of polyaniline by the scanning tunneling spectroscopy (STS) method. This effect is not as large as that observed in time-resolved fluorescence measurements for dichromophoric  $\alpha$ -helical peptides, but it should be noted that the effect of molecular dipole depends on the solvent. Our ET studies through the peptide bridges suggest that the solvation of amino acid residues by water molecules may play an important role in dampening of the molecular dipole effect.

**Acknowledgment.** This work was financially supported by MENiS funds, Project No. 120-501/68-BW-1637/14/04, and by the Ministry of Scientific Research and Information Technology, Project No. PBZ 18-KBN-098/T09/2003.

## References and Notes

- (1) Adams, D. M.; Brus, L.; Chidsey, C. E. D.; Creager, S. E.; Creutz, C.; Kagan, C. R.; Kamat, P. V.; Lieberman, M.; Lindsay, S.; Marcus, R.

- A.; Metzger, R. M.; Michel-Beyerle, M. E.; Miller, J. R.; Newton, M. D.; Rolison, D. R.; Sankey, O.; Schanze, K. S.; Yardley, J.; Zhu, X. *J. Phys. Chem. B* **2003**, *107*, 6668.
- (2) Malak, R. A.; Gao, Z.; Wishart, J. F.; Isied, S. S. *J. Am. Chem. Soc.* **2004**, *126*, 13888.
- (3) Polo, F.; Antonello, S.; Formaggio, F.; Toniolo, C.; Maran, F. *J. Am. Chem. Soc.* **2005**, *127*, 492.
- (4) Morita, T.; Kimura, S. *J. Am. Chem. Soc.* **2003**, *125*, 8732.
- (5) Bediako-Amoa, I.; Sutherland, T. C.; Li, C.-Z.; Silerova, R.; Kraatz, H.-B. *J. Phys. Chem. B* **2004**, *108*, 704.
- (6) Sek, S.; Sepiol, A.; Tolak, A.; Misicka, A.; Bilewicz, R. *J. Phys. Chem. B* **2004**, *108*, 8102.
- (7) Kraatz, H. B.; Bediako-Amoa, I.; Gyepi-Garbrah, S. H.; Sutherland, T. C. *J. Phys. Chem. B* **2004**, *108*, 20164.
- (8) Sek, S.; Moszynski, R.; Sepiol, A.; Misicka, A.; Bilewicz, R. *J. Electroanal. Chem.* **2003**, *550–551*, 359.
- (9) Kitagawa, K.; Morita, T.; Kimura, S. *J. Phys. Chem. B* **2004**, *108*, 15090.
- (10) Isied, S. S.; Ogawa, M. Y.; Wishart, J. F. *Chem. Rev.* **1992**, *92*, 381.
- (11) Petrov, E. G.; May, V. *J. Phys. Chem. A* **2001**, *105*, 10176.
- (12) Zheng, Y. J.; Case, M. A.; Wishart, J. F.; McLendon, G. L. *J. Phys. Chem. B* **2003**, *107*, 7288.
- (13) Galka, M. M.; Kraatz, H. B. *ChemPhysChem* **2002**, *3*, 356.
- (14) Williamson, D. A.; Bowler, B. E. *J. Am. Chem. Soc.* **1998**, *120*, 10902.
- (15) Skourtis, S. S.; Beratan, D. N. *J. Biol. Inorg. Chem.* **1997**, *2*, 378.
- (16) Williams, R. J. P. *J. Biol. Inorg. Chem.* **1997**, *2*, 373.
- (17) de Rege, P. J. F.; Williams, S. A.; Therien, M. J. *Science* **1995**, *269*, 1409.
- (18) Galoppini, E.; Fox, M. A. *J. Am. Chem. Soc.* **1996**, *118*, 2299.
- (19) Yasutomi, S.; Morita, T.; Imanishi, Y.; Kimura, S. *Science* **2004**, *304*, 1944.
- (20) Porter, M. D.; Bright, T. B.; Allara, D. L.; Chidsey, C. E. D. *J. Am. Chem. Soc.* **1987**, *109*, 3559.
- (21) Dubois, L. H.; Nuzzo, R. G. *Annu. Rev. Phys. Chem.* **1992**, *43*, 437.
- (22) Son, S. H.; Hong, B. H.; Lee, C.-W.; Yun, S.; Kim, K. S. *J. Am. Chem. Soc.* **2001**, *123*, 514.
- (23) Miura, Y.; Kimura, S.; Imanishi, Y.; Umemura, J. *Langmuir* **1998**, *14*, 6935.
- (24) Kennedy, D. F.; Chrisma, M.; Chapman, T. D. *Biochemistry* **1991**, *30*, 6541.
- (25) Maximum coverage for electroactive polyaniline was estimated from the charge associated with the oxidation of ferrocene redox sites. The charge was determined from cyclic voltammetric curves recorded for one-component SAM of Fc-(Ala)<sub>14</sub>NH-(CH<sub>2</sub>)<sub>2</sub>-SH.
- (26) Janek, R. P.; Fawcett, W. R.; Ulman, A. *J. Phys. Chem. B* **1997**, *101*, 8550.
- (27) Sek, S.; Bilewicz, R. *J. Electroanal. Chem.* **2001**, *509*, 11.
- (28) Finklea, H. O. Electrochemistry of Organized Monolayers of Thiols and Related Molecules on Electrodes. In *Electroanalytical Chemistry*; Bard, A. J., Rubinstein, I., Eds.; Dekker: New York, 1996; pp 109–335.
- (29) Marcus, R. A.; Sutin, N. *Biochim. Biophys. Acta* **1985**, *811*, 265.
- (30) The distance between the ferrocene moiety and sulfur atom was calculated using HyperChem 6.0. It was assumed that the structure of the polyaniline part is helical with the following dihedral angles:  $\omega = 180^\circ$ ,  $\phi = -58^\circ$ , and  $\psi = -47^\circ$ .
- (31) Sek, S.; Palys, B.; Bilewicz, R. *J. Phys. Chem. B* **2002**, *106*, 5907.
- (32) Robinson, D. B.; Chidsey, C. E. D. *J. Phys. Chem. B* **2002**, *106*, 10706.
- (33) Fox, M. A.; Galoppini, E. *J. Am. Chem. Soc.* **1997**, *119*, 5277.
- (34) To obtain the nonelectroactive derivative of polyaniline, cleavage of the desired product from the portion of resin was performed before the ferrocenecarboxylic acid coupling reaction was carried out.
- (35) Widrig, C. A.; Chung, C.; Porter, M. D. *J. Electroanal. Chem.* **1991**, *310*, 335.
- (36) Fan, F.-R. F.; Yang, J.; Cai, L.; Price, D. W.; Dirk, S. M.; Kosynkin, D. V.; Yao, Y.; Rawlett, A. M.; Tour, J. M.; Bard, A. J. *J. Am. Chem. Soc.* **2002**, *124*, 5550.
- (37) Kasibhatla, R. S. T.; Labonte, A. P.; Zahid, F.; Reifenberger, R. G.; Datta, S.; Kubiak, C. P. *J. Phys. Chem. B* **2003**, *107*, 12378.